Joint carrier and clock recovery for QPSK and MSK digital communications

Prof. E. Del Re
R. Fantacci, PhD

Indexing terms: Digital communication systems, Phasing and phase control, Satellite links, Signal processing, Detection

Abstract: A new digital implementation of a receiver for digital communications is presented. The receiver structure performs the integration of a maximum *a posteriori* probability (MAP) carrier and clock synchronisation with the maximum likelihood (ML) demodulation. It is shown that the key feature of the receiver structure is that the same hardware is able to perform both operations; thus the receiver implementation complexity is greatly reduced. This scheme can be adapted to different modulation techniques suitable for digital communications, such as QPSK, O-QPSK and MSK. As examples, the application to QPSK and MSK signals is considered, owing to the interest of these modulation schemes for satellite communications.

1 Introduction

The use of digital modulation techniques depends rather critically on the design of the synchronisation circuit employed to estimate the receiver carrier phase and bit synchronisation reference from the received signal. This paper presents the use of digital signal processing for the implementation of a coherent demodulator which integrates the carrier and clock recovery processes and which is suitable for digital communications, for instance, in regenerative satellites. A maximum *a posteriori* probability (MAP) method is used to jointly estimate the particular parameters that require synchronisation. Coherent demodulation is carried out using the maximum likelihood (ML) estimation method, which usually requires typical correlator circuits and, in some applications, a trellis decoder [1]. It is shown in this paper that, by a suitable choice of architecture for the digital coherent receiver, the ML demodulator can be easily integrated in a combined carrier and clock recovery circuit with no increase in overall system complexity. The digital architecture of the receiver can be adapted to different digital modulation techniques. Therefore, we focus here only on its application to MSK and QPSK signals, since these modulation schemes are of particular interest in satellite communications. The overall number of multiplications and additions for the coherent demodulation of MSK and QPSK signals is evaluated; then, the steady-state root-mean-square (RMS) errors of the estimated synchronisation parameters against the signal-to-noise ratio are presented for the two modulation techniques.

Paper 6679I (E8), first received 29th June 1987 and in revised form 16th January 1989

The authors are with the Dipartimento di Ingegneria Elettronica, Università di Firenze, Via S. Marta 3, 50139 Firenze, Italy

2 Integrated MAP synchronisation and ML demodulation for MSK signals

A transmitted signal of the MSK type can be written as [2]:

$$s(t) = \Sigma_n d_{I,n} \sqrt{\frac{2E}{T}}\, u[2\pi f_c(t - nT) + \psi] \times \cos\left(\frac{\pi t}{2T} + \psi\right) \cos(2\pi f_c t + \theta) + \Sigma_n d_{Q,n} \sqrt{\frac{2E}{T}}\, u[2\pi f_c(t - nT + T) + \psi] \times \sin\left(\frac{\pi t}{2T} + \psi\right) \sin(2\pi f_c t + \theta) \quad (1)$$

where $d_{I,n}(t)$ and $d_{Q,n}(t)$ are data sequences for the in-phase and quadrature channels, respectively, which are related to the input bit data sequence and are equal to ± 1 with the same probability. The function $u(x)$ is a rectangular pulse such that $u(x) = 1$ for $-\pi/2 \le x \le \pi/2$ and zero otherwise. The terms $\cos(\pi t/2T + \psi)$ and $\sin(\pi t/2T + \psi)$ represent sinusoidal weighting factors: $1/T = R$ is the signal bit rate, f_c is the carrier frequency (equal to $1/4T$) and E is the energy per bit. The carrier phase θ is a random variable which is assumed to be uniformly distributed on the interval $[-\pi, \pi]$, and ψ is the bit synchronisation phase which is assumed to be independent of θ and uniformly distributed on the interval $[-\pi/2, \pi/2]$. Now let us assume that the received signal consists of $s(t)$ plus band-limited Gaussian noise. The noise spectrum is considered to be flat and equal to $N_0/2$ (W/Hz) in the signal bandwidth $f_c - B$ to $f_c + B$, where we assume $B < f_c$. Thus

$$r(t) = s(t) + n(t) \quad (2)$$

The signal $r(t)$ supplied to the input of the digital receiver is sampled according to the Shannon sampling theorem at the rate $1/t_s = f_s$. The system, which jointly estimates the carrier phase θ and clock phase ψ, processes a block of samples r of prefixed length. A MAP method [1] is used in order to estimate simultaneously θ and ψ. The maximum *a posteriori* (MAP) estimate of θ and ψ consists of choosing $\hat{\theta}$ and $\hat{\psi}$ such that the *a posteriori* density of θ and ψ given the vector $\boldsymbol{r}$, i.e. $f(\theta, \psi/\boldsymbol{r})$, is maximised. In the following the function $f(x)$ is defined to be the probability density function (PDF) of the random variable x. If the joint probability density function $f(\theta, \psi)$ is uniform and the received signal PDF $f(\boldsymbol{r})$ is independent of θ and ψ, then from the Bayes theorem the MAP estimation procedure becomes: choose $\hat{\theta} = \theta$ and $\hat{\psi} = \psi$ such that $f(\boldsymbol{r}/\theta, \psi)$ is maximum. In order to evaluate the density $f(\boldsymbol{r}/\theta, \psi)$ we write $\boldsymbol{r}$ as the sum of a signal vector plus noise vector, i.e.

$$\boldsymbol{r} = \boldsymbol{s} + \boldsymbol{n} \tag{3}$$

The components of vectors $\boldsymbol{s}$ and $\boldsymbol{n}$ are just samples of the time waveforms $s(t)$ and $n(t)$ in accordance with the Shannon theorem. The components of the vector $\boldsymbol{n}$ are statistically independent zero-mean Gaussian random variables with variances of $N_0 B$. Thus the density $f(\boldsymbol{r} \mid \theta, \psi)$ can be written as [3]:

$$\begin{aligned} f(\boldsymbol{r} \mid \theta, \psi) = C_0(\boldsymbol{r}) \prod_{i=1}^{L+1} \cosh \Bigg[\frac{2t_s}{N_0} \sqrt{\frac{2E}{T}} \sum_{k=1}^{N} r(t) \\ \times \cos\left(\frac{\pi t}{2T} + \hat{\psi}\right) \cos(2\pi f_c t + \hat{\theta}) \Bigg] \Bigg|_{t=(2i-1)T + kt_s - 2\hat{\psi}T/\pi} \\ \times \prod_{i=0}^{L+1} \cosh \Bigg[\frac{2t_s}{N_0} \sqrt{\frac{2E}{T}} \sum_{k=1}^{N} r(t) \\ \times \sin\left(\frac{\pi t}{2T} + \hat{\psi}\right) \sin(2\pi f_c t + \hat{\theta}) \Bigg] \Bigg|_{t=2iT + kt_s - 2\hat{\psi}T/\pi} \end{aligned} \tag{4}$$

where $C_0(\boldsymbol{r})$ is a term which is not depended on θ and ψ, $2(L + 2)$ is the number of intervals (each T long) required to estimate θ and ψ, and N is the number of samples per symbol. A necessary but not sufficient condition that must be satisfied by $\hat{\theta}$ and $\hat{\psi}$ in order to be MAP estimates of θ and ψ is given by Booth [3] with reference to an analogue implementation. The corresponding digital version of the MAP carrier and clock estimator is [4]:

$$\begin{aligned} \frac{\partial \ln f(\boldsymbol{r} \mid \theta, \psi)}{\partial \theta}\Bigg|_{\substack{\theta=\hat{\theta} \\ \psi=\hat{\psi}}} = -\Bigg\{ \sum_{i=1}^{L+1} \tanh \Bigg[\frac{2t_s}{N_0} \sqrt{\frac{2E}{T}} \sum_{k=1}^{N} r(t) \\ \times \cos\left(\frac{\pi t}{2T} + \hat{\psi}\right) \cos(2\pi f_c t + \hat{\theta}) \Bigg] \\ \times \sum_{k=1}^{N} \Bigg[r(t) \cos\left(\frac{\pi t}{2T} + \hat{\psi}\right) \\ \times \sin(2\pi f_c t + \hat{\theta}) \Bigg] \Bigg\} \Bigg|_{t=(2i-1)T + kt_s - 2\hat{\psi}T/\pi} \\ + \Bigg\{ \sum_{i=0}^{L+1} \tanh \Bigg[\frac{2t_s}{N_0} \sqrt{\frac{2E}{T}} \sum_{k=1}^{N} r(t) \\ \times \sin\left(\frac{\pi t}{2T} + \hat{\psi}\right) \sin(2\pi f_c t + \hat{\theta}) \Bigg] \\ \times \sum_{k=1}^{N} r(t) \sin\left(\frac{\pi t}{2T} + \hat{\psi}\right) \\ \times \cos(2\pi f_c t + \hat{\theta}) \Bigg\} \Bigg|_{t=2iT + kt_s - 2\hat{\psi}T/\pi} = 0 \end{aligned} \tag{5a}$$

$$\begin{aligned} \frac{\partial \ln f(\boldsymbol{r} \mid \theta, \psi)}{\partial \psi}\Bigg|_{\substack{\theta=\hat{\theta} \\ \psi=\hat{\psi}}} = -\Bigg\{ \sum_{i=1}^{L+1} \tanh \Bigg[\frac{2t_s}{N_0} \sqrt{\frac{2E}{T}} \sum_{k=1}^{N} r(t) \\ \times \cos\left(\frac{\pi t}{2T} + \hat{\psi}\right) \cos(2\pi f_c t + \hat{\theta}) \Bigg] \\ \times \sum_{k=1}^{N} r(t) \sin\left(\frac{\pi t}{2T} + \hat{\psi}\right) \\ \times \cos(2\pi f_c t + \hat{\theta}) \Bigg\} \Bigg|_{t=(2i-1)T + kt_s - 2\hat{\psi}T/\pi} \\ + \Bigg\{ \sum_{i=0}^{L+1} \tanh \Bigg[\frac{2t_s}{N_0} \sqrt{\frac{2E}{T}} \sum_{k=1}^{N} r(t) \\ \times \sin\left(\frac{\pi t}{2T} + \hat{\psi}\right) \sin(2\pi f_c t + \hat{\theta}) \Bigg] \\ \times \sum_{k=1}^{N} r(t) \cos\left(\frac{\pi t}{2T} + \hat{\psi}\right) \\ \times \sin(2\pi f_c t + \hat{\theta}) \Bigg\} \Bigg|_{t=2iT + kt_s - 2\hat{\psi}T/\pi} = 0 \end{aligned} \tag{5b}$$

These equations can be considered as error signals; thus, the MAP estimate of θ at the instant $(k + 1)T$, i.e. $\hat{\theta}_{k+1}$, and the MAP estimate of ψ at the instant $(k + 1)T$, i.e. $\hat{\psi}_{k+1}$ can be evaluated according to

$$\begin{aligned} \hat{\theta}_{k+1} = \hat{\theta}_k + k_\theta \frac{\partial \ln f(\boldsymbol{r} \mid \theta, \psi)}{\partial \theta}\Bigg|_{\substack{\theta=\hat{\theta} \\ \psi=\hat{\psi}}} \\ \hat{\psi}_{k+1} = \hat{\psi}_k + k_\psi \frac{\partial \ln f(\boldsymbol{r} \mid \theta, \psi)}{\partial \psi}\Bigg|_{\substack{\theta=\hat{\theta} \\ \psi=\hat{\psi}}} \end{aligned} \tag{6}$$

where k_θ is the carrier loop gain and k_ψ is the clock loop gain. These parameters must be determined in order to guarantee both system stability and good tracking performance. The configuration of the digital system which jointly estimates θ and ψ as suggested by eqns. 5*a* and 5*b* is depicted in Fig. 1. The carrier and clock recovery circuit previously described can be affected by a 180° ambiguity for θ; to escape a high bit-error rate, suitable differential encoding should be introduced in the modulation scheme. Indeed, differential encoding is inherent in the MSK signal. Moreover, a better performance is achieved by employing an ML detection method with respect to classical quadrature demodulation followed by differential decoding [2]. In a classical ML demodulator the correlations between the received waveform and each of the possible signals represent the metrics to be evaluated. Over an appropriate number of bit intervals these metrics are accumulated and used to detect the first transmitted bit, i.e. the first bit of the sequence corresponding to the largest metric. In the case of MSK signals, the optimum observation interval is equal to two bits [2]. The digital receiver architecture can be adapted to integrate the ML detection circuit with the joint MAP carrier and clock recovery circuit as shown in Fig. 1. The product of $r(t)$ and two possible transmitted signals $\cos(2\pi f_c t \pm \pi t/2T)$ is derived at the points A and A′ of Fig. 1, by exploiting well-known trigonometric identities. Thus, a substantial reduction in receiver implementation complexity is obtained with respect to a classical receiver scheme, in which the operations of carrier and clock recovery and coherent demodulation are performed separately.

3 Integrated MAP synchronisation and ML demodulation for QPSK signals

The QPSK signal can be written as

$$s(t) = \sqrt{\frac{2E}{T}} \sum_i [d_I(i)p(t - 2iT + \varepsilon) \times \cos(2\pi f_c t + \theta) + d_Q(i)p(t - 2iT + \varepsilon) \times \sin(2\pi f_c t + \theta)] \quad (7)$$

where θ is the random carrier phase, which is assumed to be uniformly distributed on the interval $[-\pi, \pi]$, ε is the random bit synchronisation time, which is assumed to be independent of θ and unformly distributed on the interval $[-T, T]$, $d_I(i)$ is the inphase data sequence and $d_Q(i)$ is the quadrature data sequence. The $d_I(i)$ and $d_Q(i)$ are independent random variables, which can assume the values ± 1 with equal probability. The function $p(x)$ is a rectangular function defined as:

$$p(x) = \begin{bmatrix} 1, & 0 < x < 2T \\ 0, & \text{otherwise} \end{bmatrix} \quad (8)$$

Now assume the same hypothesis for the MSK case. The density $f(r/\theta, \varepsilon)$ can be written as:

$$f(\mathbf{r} \mid \theta, \varepsilon) = C_0'(\mathbf{r}) \left\{ \prod_{i=0}^{L} \cosh \left[\frac{2t_s}{N_0} \sqrt{\frac{2E}{T}} \times \sum_{k=1}^{N} r(t)p(t - iT + \hat{\varepsilon}) \cos(2\pi f_c t + \hat{\theta}) \right] \times \prod_{i=0}^{L} \cosh \left[\frac{2t_s}{N_0} \sqrt{\frac{2E}{T}} \prod_{k=1}^{N} r(t)p(t - iT + \hat{\varepsilon}) \times \sin(2\pi f_c t + \hat{\theta}) \right] \right\} \Bigg|_{t = 2T + kt_s} \quad (9)$$

where $L + 1$ is the number of intervals (each $2T$ long) used to estimate θ and ε, N is the number of samples per symbol time and $C_0(\mathbf{r})$ is a term independent of θ and ε. In the same manner a necessary, but not sufficient, criterion that must be satisfied by $\hat{\theta}$ and $\hat{\varepsilon}$ in order to be the MAP estimates of θ and ε must be determined as:

$$\frac{\partial \ln f(\mathbf{r} \mid \theta, \varepsilon)}{\partial \theta} \Bigg|_{\substack{\theta = \hat{\theta} \\ \varepsilon = \hat{\varepsilon}}} = -\left\{ \sum_{i=0}^{L} \tanh \left[\frac{2t_s}{N_0} \sqrt{\frac{2E}{T}} \times \sum_{k=1}^{N} r(t)p(t - iT + \hat{\varepsilon}) \cos(2\pi f_c t + \hat{\theta}) \right] \times \sum_{k=1}^{N} r(t)p(t - iT + \hat{\varepsilon}) \sin(2\pi f_c t + \hat{\theta}) + \sum_{i=0}^{L} \tanh \left[\frac{2t_s}{N_0} \sqrt{\frac{2E}{T}} \sum_{k=1}^{N} r(t)p(t - iT + \hat{\varepsilon}) \times \sin(2\pi f_c t + \hat{\theta}) \right] \sum_{k=1}^{N} r(t)p(t - iT + \hat{\varepsilon}) \times \cos(2\pi f_c t + \hat{\theta}) \right\} \Bigg|_{t = iT + kt_s\hat{\varepsilon}} = 0 \quad (10a)$$

$$\frac{\partial \ln f(\mathbf{r} \mid \theta, \varepsilon)}{\partial \varepsilon} \Bigg|_{\substack{\theta = \hat{\theta} \\ \varepsilon = \hat{\varepsilon}}} = -\left\{ \sum_{i=0}^{L} \tanh \left[\frac{2t_s}{N_0} \sqrt{\frac{2E}{T}} \times \sum_{k=1}^{N} r(t)p(t - iT + \hat{\varepsilon}) \cos(2\pi f_c t + \hat{\theta}) \right] \right\} \Bigg|_{t - iT + kt_s\hat{\varepsilon}} \times \left[r(t) \cos(2\pi f_c t + \hat{\theta}) \big|_{t = iT - \hat{\varepsilon}} - r(t) \right.$$

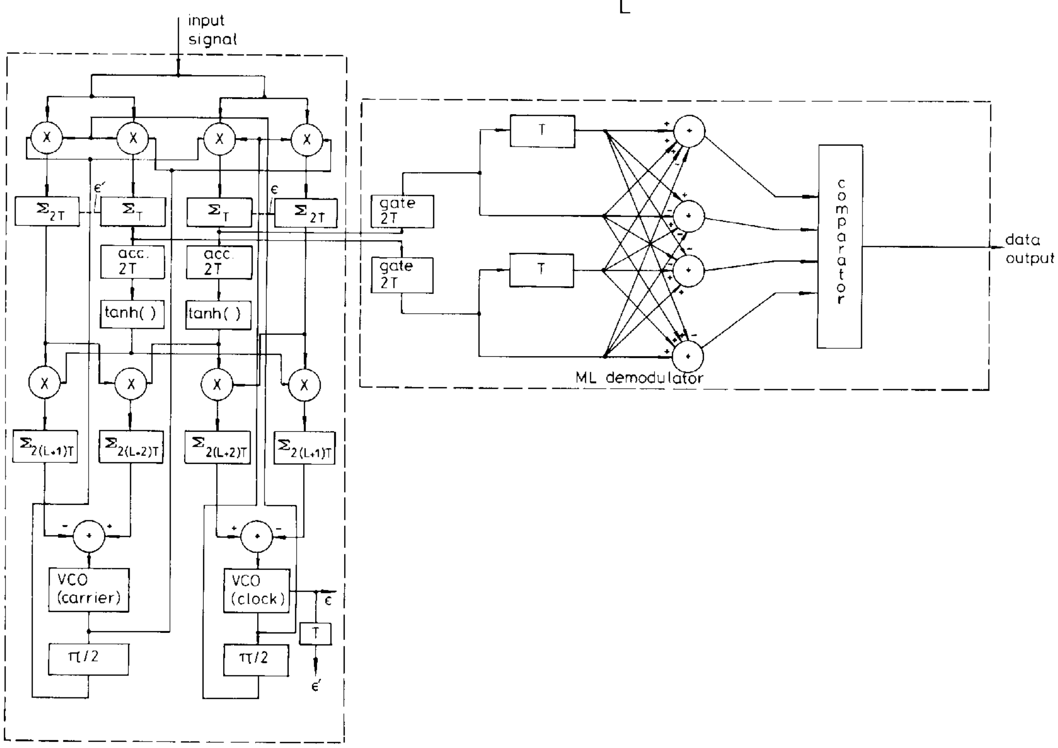

Fig. 1 *Block diagram of digital communication receiver with integrated MAP synchronisation and ML demodulation for MSK signal*

$$\times \cos(2\pi f_c t + \hat{\theta})\Big|_{t=(i+1)T-\hat{\varepsilon}}\Bigg]$$

$$+ \left\{\sum_{i=0}^{L} \tanh\left[\frac{2t_s}{N_0}\sqrt{\frac{2E}{T}}\sum_{k=1}^{N} r(t)p(t - iT + \hat{\varepsilon})\right.\right.$$

$$\left.\times \sin(2\pi f_c t + \hat{\theta})\right\}\Bigg|_{t=iT+kt_s\hat{\varepsilon}}$$

$$\times \left[r(t)\sin(2\pi f_c t + \hat{\theta})\Big|_{t=iT-\hat{\varepsilon}} - r(t)\right.$$

$$\left.\times \sin(2\pi f_c t + \hat{\theta})\Big|_{t=(i+1)T-\hat{\varepsilon}}\right] = 0 \qquad (10b)$$

These equations can be considered as error signals; then $\hat{\theta}_{k+1}$ and $\hat{\varepsilon}_{k+1}$ are obtained as in eqn. 6. The configuration of the digital system which jointly estimates θ and ε for QPSK signals, as suggested by eqns. 10*a* and 10*b*, is shown in Fig. 2. In this application the carrier and clock recovery circuit can be affected by a 90° ambiguity in θ; therefore, a suitable differential encoding process should be introduced into the modulation scheme. The ML demodulator for QPSK signals can be integrated with the combined carrier and clock recovery circuit with no increase in overall system complexity. In a coherent demodulator for QPSK signals the product of $r(t)$ with the two quadrature carriers $\cos(2\pi f_c t)$ and $\sin(2\pi f_c t)$ must be evaluated. In the digital receiver architecture shown in Fig. 2, these two products can be derived at the points B and B′; then, the same hardware is able to perform both the operations of combined carrier and clock recovery and coherent demodulation with a substantial reduction in receiver implementation complexity.

The integration of the ML demodulator in the MAP synchronisation circuit is an important feature when the main goal is implementation complexity reduction. In particular, the proposed synchronisation approach represents a suitable solution for application in advanced digital satellite communication systems. An example is given in Reference 5.

4 Results and conclusions

The overall number of multiplications and additions for the coherent demodulation of MSK and QPSK signals have been evaluated, and the steady-state RMS errors of the estimated phases of the carrier and clock as a function of the parameter E/N_0 have been determined.

Coherent demodulation of MSK signals is considered first. The overall number of multiplications and additions required by the proposed digital receiver with integrated MAP synchronisation and ML demodulation is given by:

$$M_{MSK} = 2(3N + 2)(L + 1) + 3N + 2 \quad \text{multiplications/symbol}$$

$$S_{MSK} = 4N(L + 1) + 2(N - 1) \quad \text{additions/symbol} \qquad (11)$$

In Fig. 3, the steady-state RMS errors of the estimated phase of the carrier and clock are shown against the parameter E/N_0. The results have been derived through simulations. It is evident from Fig. 3 that the MAP carrier and clock recovery circuit achieves a very good

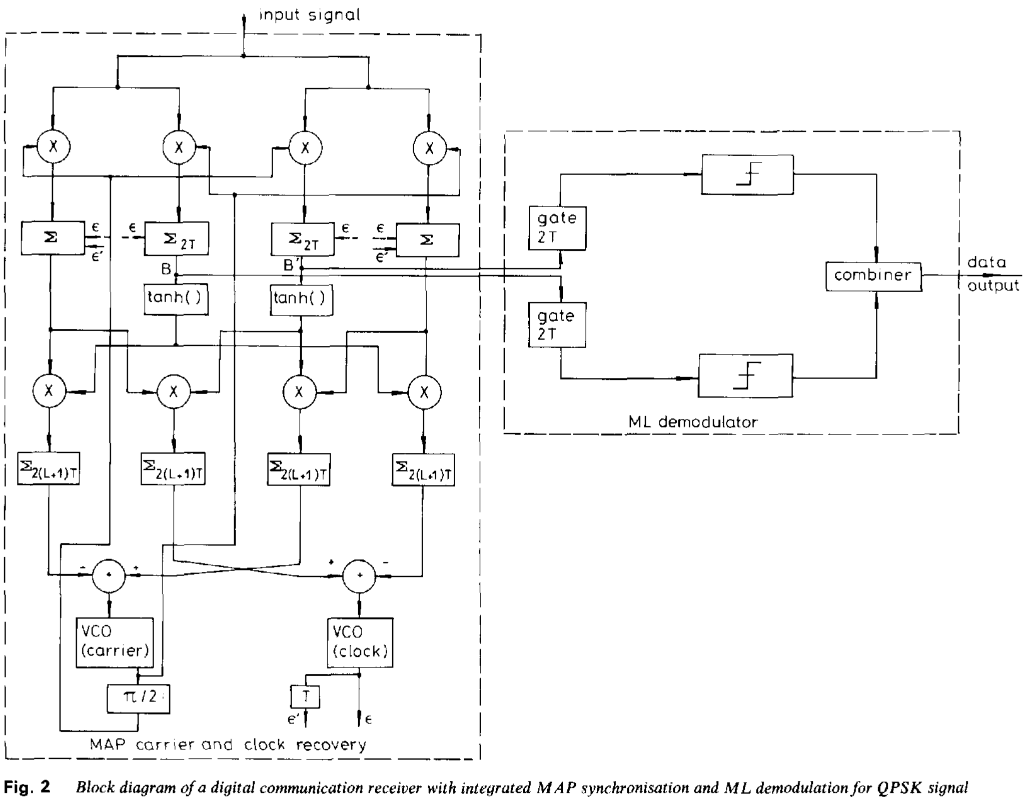

Fig. 2 *Block diagram of a digital communication receiver with integrated MAP synchronisation and ML demodulation for QPSK signal*

synchronisation performance that guarantees a negligible (less than 0.2 dB) degradation in the obtainable bit error rate for high signal-to-noise ratios.

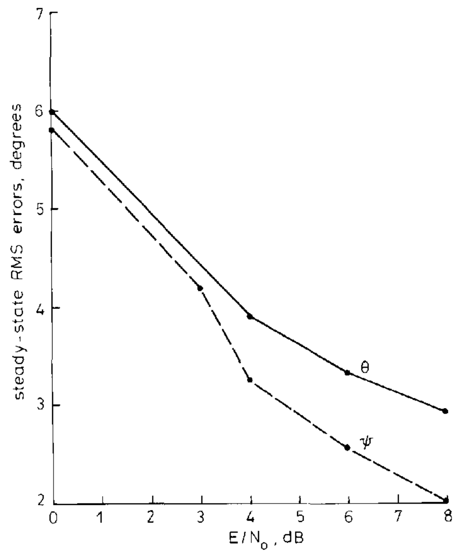

Fig. 3 *Steady-state RMS errors of carrier (θ) and clock (ψ) estimated phases against E/N_0 for MSK signal*
$L = 2, N = 3$

The overall number of multiplications and additions for coherent demodulation of QPSK signals by a digital receiver with integrated MAP synchronisation and ML demodulation has been evaluated as:

$$M_{QPSK} = 2(N + 4)(L + 1) \quad \text{multiplications/symbol}$$
$$S_{QPSK} = (2N + 1)(L + 1) + 3L + 1 \quad \text{additions/symbol} \tag{12}$$

In Fig. 4 the steady-state RMS error in the carrier phase is shown against the parameter E/N_0. In the same figure the parameter Δ, i.e. the RMS error in clock time referred to the symbol time $2T$ and expressed as a percentage, is also shown as a function of E/N_0.

From Fig. 4, it can be seen that the RMS steady-state clock-timing error (curve Δ) decreases at a slower rate than the RMS steady-state carrier phase error (curve θ). A different behaviour is shown in Fig. 3 for the MSK signal. This can be explained by recalling that, for the QPSK signal, a rectangular pulse-shaping has been considered. Therefore, as explained in more detail in Reference 5, the resulting QPSK signal can be more tolerant to timing errors than MSK.

Fig. 4 shows that the MAP carrier and clock recovery circuit achieves a very good tracking performance and introduces a negligible (less than 0.1 dB) degradation in the overall bit error rate for high signal-to-noise ratios.

Finally, it can be concluded that the proposed digital receivers with integrated MAP synchronisation and ML demodulation for MSK and QPSK signals achieve a good synchronisation performance without increasing the overall system complexity. Therefore the combination of an integrated MAP synchronising circuit and an ML demodulator for both MSK and QPSK signals is highly suitable for custom or semicustom VLSI implementation.

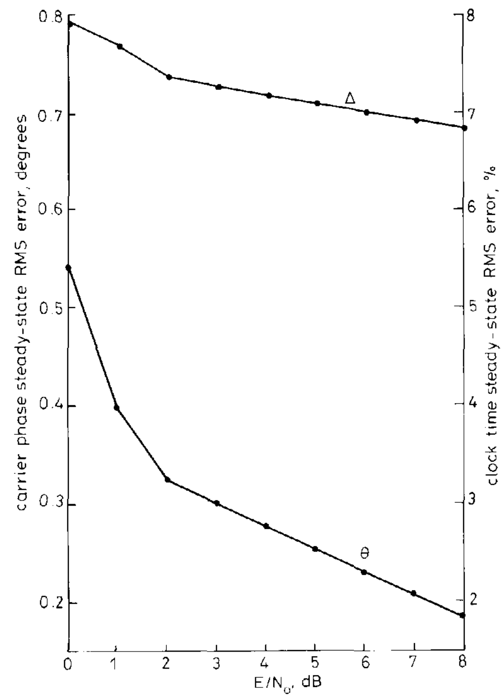

Fig. 4 *Steady-state RMS error of carrier (θ) estimated phase and steady-state RMS error of clock (Δ) estimated time as percentage against E/N_0 for QPSK signal*
$L = 2, N = 3$

5 Acknowledgment

The work reported in this paper was supported by the Ministero Pubblica Istruzione, Italy.

6 References

1. VAN TREES, H.L.: 'Detection, estimation and modulation theory' (Wiley, New York, 1968)
2. BHARGAVA, V.K., HACCAUN, D., MATYAS, R., and NUSPL, P.P.: 'Digital communication by satellite' (Wiley, New York, 1984)
3. BOOTH, R.W.: 'An illustration of the MAP estimation method for deriving closed-loop phase tracking topologies: the MSK signal structure', *IEEE Trans.*, 1980, **COM-28**, pp. 1137–1142
4. DEL RE, E., and FANTACCI, R.: 'A digital communication receiver with integrated MAP synchronisation and ML demodulation', *Electron. Lett.*, 1985, **21**, pp. 862–864
5. DEL RE, E., and FANTACCI, R.: 'Multicarrier demodulator for digital satellite communication systems', *IEE Proc. I, Commun., Speech & Vision*, 1989, **136**, pp. 201–207